Automated Quality Assurance of CFRP-Components Using Air-Coupled Ultrasound

Armin Huber

***Abstract*—To this day, carbon fiber reinforced plastic (CFRP)-components are used in aerospace only to a minor degree, because its fabrication is much more expensive than production of metallic components, which is due to the high amount of handcraft that is involved. Therefore, it is the aim of the German Aerospace Center to automate the production process of CFRP by using robots. An important part of the production process is quality assurance. One of the methods that are used at DLR is non-destructive inspection (NDI) by using air-coupled ultrasonic testing (ACU-testing). In contrast to water-coupled ultrasonic testing, this method is completely contactless and allows for inspection of CFRP-components with high amount of porosity of a few percent. ACU-testing is going to be automated as well and, in another effort, be integrated into the automated production process. The acquired data from ACU-testing could then be used for optimization of the production process. Despite its high potential as an NDI-method, ACU-testing facilities for reflection measurements exist only in laboratories. Thus, it is another aim of DLR to improve the method to a degree, where it can be introduced into industrial sites. For this purpose, reflection measurements on test components and a pressure vessel were carried out with an ACU-testing device. In the course of those experiments the degree of automation of the NDI-method was increased step by step.**

***Index Terms*—NDI, ultrasonic, guided waves, composites, delamination detection, robot, offline programming, path-equidistant triggering**

I. Introduction

WATER-coupled ultrasonic testing is part of the quality assurance in aerospace and automotive industry for many years. On the other hand, air-coupled ultrasonic testing is not applied to the same extent to this day. However, facilities for transmission measurements exist in the industry. For instance, Airbus Helicopters Germany, München has established a facility for ACU-testing in transmission only in 2011 [1]. Reflection mode is available only on laboratory scale like at the Institut für Kunststofftechnik of Universität Stuttgart, where it is used for fatigue monitoring of composite tubes [2]. In fact, ACU-testing in reflection, which works by excitation of so-called plate- or guided waves in the component to be tested, would be desirable for industrial application in cases where only single-sided access to the component is available. The benefits of ACU-testing are obvious. One can abstain from all infrastructure that is related to the coupling medium water like immersion tanks, tubes, water conditioning etc. Furthermore, robots and electrical equipment are not affected by moisture and no water will infiltrate the CFRP-components or cause corrosion. Crucial parameters known from water-coupled ultrasonic testing like contact pressure and flow rate of the coupling medium (possibility of loosing contact) are non-relevant. Also, CFRP with a high amount of porosity like thermoplastics can be inspected, where water-coupled ultrasound gets scattered easily due its shorter wavelengths. Although Luukkala et al. succeeded in exciting plate waves and detecting flaws in aluminum already in the 1970's [3], and despite their recommendation to use this technique for 'on-line' testing, no try was undertaken to industrialize ACU-testing in reflection so far. One reason for this is the large mismatch of the acoustic impedances of air and the material to be tested. Consequently, there is a low transmission coefficient for ultrasound transmitting through the interface between air and metal or CFRP. For instance, only $0.005\,\%$ of ultrasound transmit through the interface air/aluminum compared to approximately $16\,\%$ transmitting through the interface water/aluminum (calculation based on [4, p. 48]). To solve this problem, improvements were achieved in the field of electronics (digital filters, amplification etc.), new piezo-composite materials for transducers with reduced acoustic impedance [5] and $\lambda/4$-coatings to reduce destructive interferences [6]. Of course, significant progress has also been achieved in the field of computer development and electronic data processing.

As far as process automation is concerned, the application of robots is state of the art. Therefore, it is advisable to use robots for automation of quality assurance processes, too. Flexibility and range of robots allow for scanning of large and curved components with a targeted coverage of its surface of $100\,\%$. Around five to ten years ago robots lacked the required accuracy. They were programmed by teaching in order to repeat certain - not to complex - motions unlimited times. Since then robots have to perform more and more complex programs, which can only be created by offline programming (OLP). In the past few years the accuracy could be improved far enough to allow for scanning of complex shapes. As shown in this paper, path-equidistant triggering of sensors (like ultrasonic transducers) by the robot control unit is now possible with high precision and repetition frequency. These technical achievements have to keep pace with the increasingly demanding standards of quality assurance regarding flexibility, speed and reproducibility.

In this work, experiments are presented that were conducted with an ACU-testing device. All measurements were conducted using a robot, where the degree of integration of the ACU-testing device into the robot cell and the automation of the testing process as a whole increased from one measurement to the other.

The author is with the Institute of Structures and Design, German Aerospace Center (DLR), Augsburg, Germany, email: armin.huber@dlr.de.

II. Theory

Since the theoretical background of plate waves and their excitation is examined in [4], [7] and [8] extensively, only a brief discussion about measurement principles and the excitation of Lamb waves will follow.

A. Principles of measurement

As depicted in Fig. 1, measurements in transmission and reflection are distinguished. The pulse-echo method will not be discussed here. In transmission mode the plate to be tested is located between the ultrasonic transducers (transmitter and receiver) and causes attenuation of the ultrasound (Fig. 1a). The degree of attenuation is affected by flaws like delaminations. The transducers are mounted on a bow, which is moved by a scanner or a robot. For large and curved components two cooperating robots can be used. Through scanning the component by sound an ultrasonic picture (C-scan) is obtained. Another method is slanted incidence of the ultrasound beam (Fig. 1b). Here, so called 'plate waves' (Lamb- and Rayleigh waves) are excited. This enables detection of the Lamb waves from the side they are excited from. Therefore, single-sided access to the plate is sufficient (Fig. 1c).

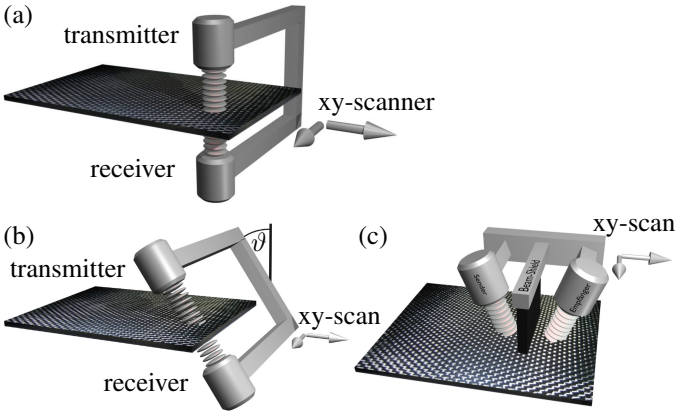

Figure 1: Measurement principles of ACU-testing [4]. (a) normal transmission mode (NTM) (b) focused slanted transmission mode (FSTM) (c) focused slanted reflection mode (FSRM)

B. Excitation of Lamb waves

Consider an isotropic plate, which is exposed to an ultrasonic beam with an incidence angle ϑ. Let the beam propagate through air with a wave vector $\boldsymbol{k}_\mathrm{a}$ and the phase velocity v_a. In order to excite a Lamb wave with wave vector $\boldsymbol{k}_\mathrm{l}$ and phase velocity v_l, Snell's law must be fulfilled:

$$k_\mathrm{l} = k_\mathrm{a} \sin\vartheta \tag{1}$$

Using the relation

$$k = |\boldsymbol{k}| = \frac{\omega}{v}, \tag{2}$$

where ω is the angular frequency, gives

$$\sin\vartheta = \frac{k_\mathrm{l}}{k_\mathrm{a}} = \frac{\lambda_\mathrm{a}}{\lambda_\mathrm{l}} = \frac{v_\mathrm{a}}{v_\mathrm{l}}. \tag{3}$$

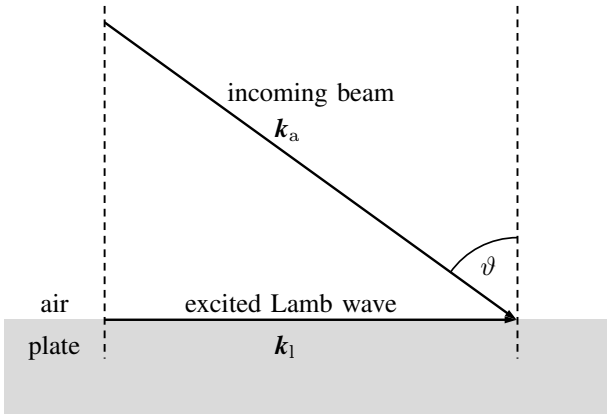

Figure 2: Diagram showing the relationship between $\boldsymbol{k}_\mathrm{a}$ and $\boldsymbol{k}_\mathrm{l}$.

As shown in Fig. 2, the geometric meaning of this is that the incidence angle must be chosen in a way that the projection on the interface air/plate of the incoming wave $\boldsymbol{k}_\mathrm{a}$ matches the excited Lamb wave $\boldsymbol{k}_\mathrm{l}$.

According to equation (3), the incidence angle depends on the ratio of the phase velocities of air and Lamb wave. Furthermore, the phase velocity of the Lamb wave is dispersive, which means that it is frequency dependent [9]. There exist numerous different modes (symmetric and antisymmetric ones), all of which are dispersive. They are displayed in dispersion diagrams like shown in [3], [10] and [11]. For the excitation of only one Lamb wave mode one should keep the frequency rather low, since there are less and better separated modes on the left in the diagrams. According to [9] and [10], excitation of the 0th order antisymmetric mode is preferred for ACU-testing in reflection mode.

When a Lamb wave is excited the plate/component is oscillating throughout its whole thickness but, of course, only in the place where it is excited and along the direction of propagation. By continuous reemission of ultrasound along the propagation path (in Fig. 3 to the right), the amplitude of the Lamb wave gets diminished gradually. Due to the high mismatch of acoustic impedances in the case of ACU, the degree of reemission is accordingly low and therefore the Lamb waves have a relatively high range of propagation in solid matter.

Most ultrasound intensity reaches the receiver directly through the air or by reflection at the air/plate interface. This

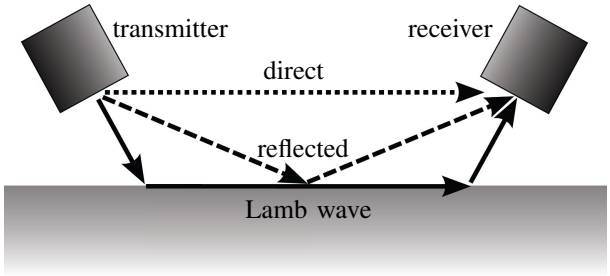

Figure 3: Propagation of ultrasound in Lamb wave mode [4].

signal can overlay the ultrasound reemitted by the Lamb waves and must be shielded by a beam shield, which is mounted between transmitter and receiver (Fig. 1c). One should note that in this configuration only the reemitted ultrasound is of interest for evaluation but not the reflected one as the nomenclature 'focused slanted *reflection* mode' implies.

III. Measurements with Lamb waves

The ACU-testing device used at DLR Augsburg was constructed by Inoson GmbH and provides the required interfaces for communication with the robotic environment and automation. Three pairs of transducers with integrated preamplifiers are available. Their frequencies are 64, 110 and 200 kHz. Those transducers are mounted on an endeffector, which in turn is fixed at the robot's flange. The robot is a construction by KUKA (KR120 R2700 extra HA) and possesses six axes. It has a particularly high repetition accuracy of approximately $\pm 0.6\,\mathrm{mm}$ and provides motion and triggering of the transducers. The function of the robot is fast and precise motion while keeping alignment (in order to keep the incidence angle stable) and distance of the transducers constant with respect to the component to be scanned.

A. Measurement of a flat plate with artificial flaws

The first measurement with Lamb waves was performed on a plate using $110\,\mathrm{kHz}$ transducers. Square-cut PTFE tape was inserted into the plate in order to simulate delaminations. The task was to check the functionality of the integrated ACU-testing device together with the robot and to achieve a C-scan that displays the artificial delaminations.

The setup is shown in Fig. 4. The plate was supported only at its edges in order to avoid damping of the Lamb waves through contact with the table below. The transducers were mounted on an endeffector, which provides adjustment of incidence- and receiving angle. A piece of cardboard was used as beam shield.

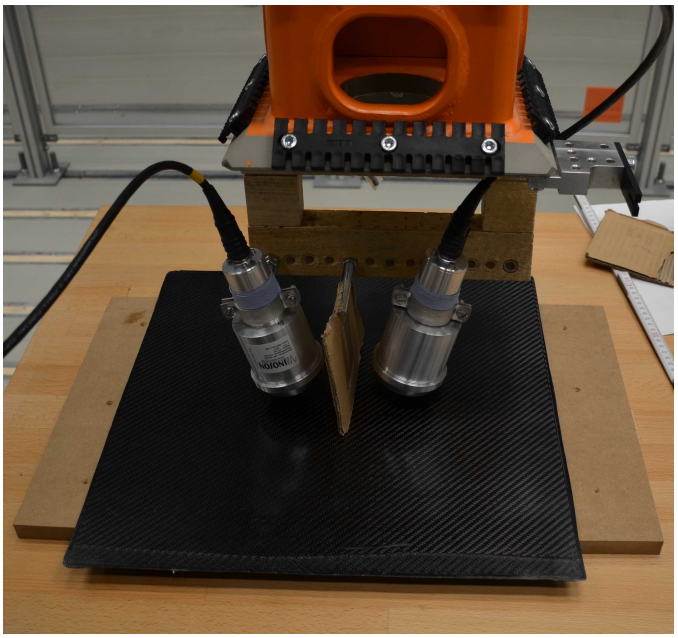

Figure 4: Measurement of a flat plate using Lamb waves. The receiver on the right is shielded against the transmitter by a piece of cardboard.

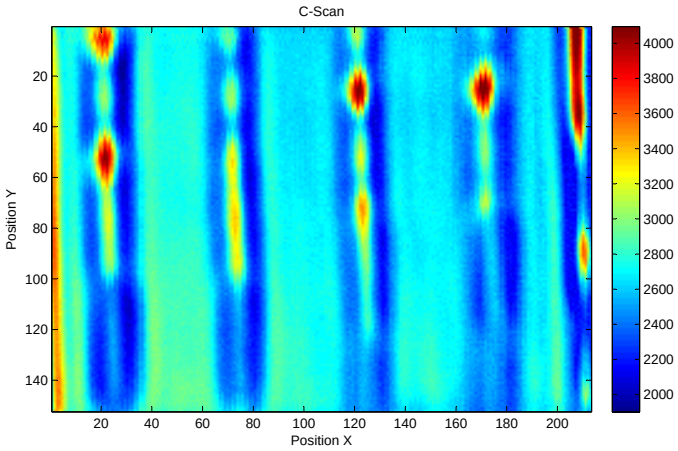

Figure 5: C-scan of the plate, obtained with $110\,\mathrm{kHz}$. The red spots indicate artificial delaminations.

The robot was taught a meander-like motion for scanning the plate. Every $2\,\mathrm{mm}$ on this path (resulting in a $2 \times 2\,\mathrm{mm}$ grid) the ACU-testing device was triggered by the robot control unit to send an ultrasonic pulse. For each ultrasonic pulse the robot had to stop before moving to the next triggering position (stop & go mode). This resulted in a pulse repetition frequency of $4\,\mathrm{Hz}$ and therefore an effective path velocity of $8\,\mathrm{mm/s}$.

Analysis and visualisation of the data has been carried out with MATLAB. Programming has been done in cooperation with the Institut für Kunststofftechnik of Universität Stuttgart. The result of the measurement is shown in Fig. 5.

Every pixel in this picture (pixel size: $2 \times 2\,\mathrm{mm}$) represents one measurement position and the colour of the pixel corresponds to the signal amplitude. The axes indicate coordinates in measurement positions. Red colour corresponds to a high Lamb wave-amplitude. Thus, delaminations seem to cause an increase of the amplitude. This can be explained as follows: The delamination divides the plate into an area above and an area below the delamination. Lamb waves will be excited only above the delamination. Exciting a thinner plate takes less energy, so the amplitude will increase. This is contrary to transmission mode measurements, where a delamination causes a decrease of the transmitted amplitude. However, in reflection mode flaws can lead to decrease as well as increase of the amplitude, depending on the type of flaw. It should also be noted that in the data obtained from reflection measurements, no information about the depth of the delamination or any kind of flaw is contained.

Moreover, it is striking that the red spots are not square as one would expect, but are distorted along the Y-direction (direction of Lamb wave-propagation). This effect can be ascribed to the large distance of $15\,\mathrm{cm}$ between the transducers. Generally, this leads to C-scans of lower quality as compared to ones obtained from transmission measurements.

It must be considered that all properties of the plate that are located on the path, which the Lamb wave passes between transmitter and receiver are accumulated and displayed in one pixel. The location of this pixel is assigned to the current coordinates of the tool center point (TCP) of the robot in an appropriate coordinate system. The TCP is located in the middle between the transducers. The distance between the transducers should be kept as small as possible in order to improve resolution and reduce distortion of features. Since all available transducers have a large housing of $7.5\,\mathrm{cm}$ diameter, this effort is hampered to some extent. Another aspect of a large transducer is that a large area of the plate is excited, which also leads to less resolution. On the other hand, their field of sound is more homogenous and more energy can be yielded into the plate. This is of particular importance when thick plates shall be excited.

B. Measurement of a demonstrator component

The next measurement with Lamb waves was conducted on a $1.4\,\mathrm{m}$ diameter demonstrator component again with $110\,\mathrm{kHz}$ transducers. The component emulates a part of a pressure vessel of a rocket booster and was constructed at the Lehrstuhl für Carbon Composites of Technische Universität München. It consists of carbon fibre thermoplastic prepregs and was fabricated by a laser based in situ consolidation winding process. It has a high amount of porosity of $2-4\,\%$, which makes it impossible for inspection using water-coupled ultrasound. As Fig. 6 shows, the demonstrator consists of a cylindric part and a dome. The task was to scan the curved geometry while keeping alignment and distance of the endeffector constant with respect to the component and obtaining C-scans of some areas.

An improvement regarding the handling of the rotationally symmetric demonstrator was mounting it on the tilt-turn table (TTT), which allows for rotation and tilting. Meander-like scanning would now be performed by rotation (completely or partly) of the demonstrator while keeping the endeffector at one position and triggering the transducers. After one rotation the TTT stops, the robot moves the endeffector up or down

Figure 6: Robot cell at DLR Augsburg with KUKA robot. The demonstrator is mounted on the tilt-turn table.

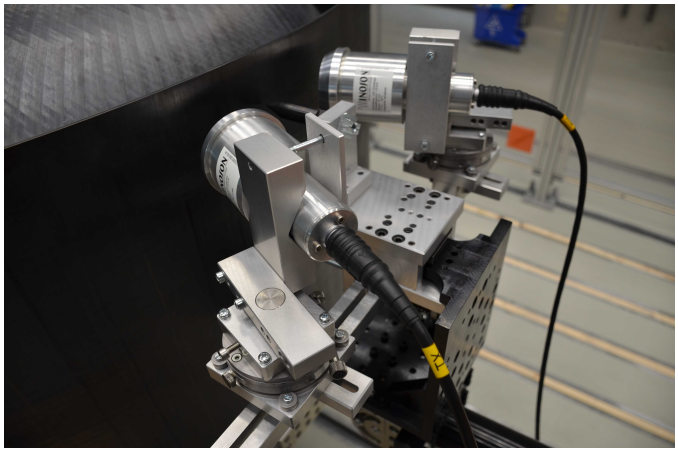

Figure 7: The new endeffector allows for reproducible adjustment of transducers in four degrees of freedom.

by one measurement position, then the TTT rotates back in the other direction and so on. This practice not only appears more elegant than complicated motions of six robot axes for conducting such a meander with the robot on a fixed demonstrator. It also allows for more coverage like the far side of the demonstrator.

Another improvement was the construction of a new endeffector, shown in Fig. 7. It provides stepless adjustment of the transducers in three translatoric and one rotatoric degrees of freedom. Attached scales enable reproducibility of the adjustment.

For the C-scan shown in Fig. 8 a $20 \times 20\,\mathrm{cm}$ area on the cylindric part of the demonstrator was scanned using a $2 \times 2\,\mathrm{mm}$ grid in stop & go mode. Accordingly, the TTT performed clockwise and anticlockwise $17\,^\circ$ rotations alternately. Again a pulse repetition frequency of $4\,\mathrm{Hz}$ and an

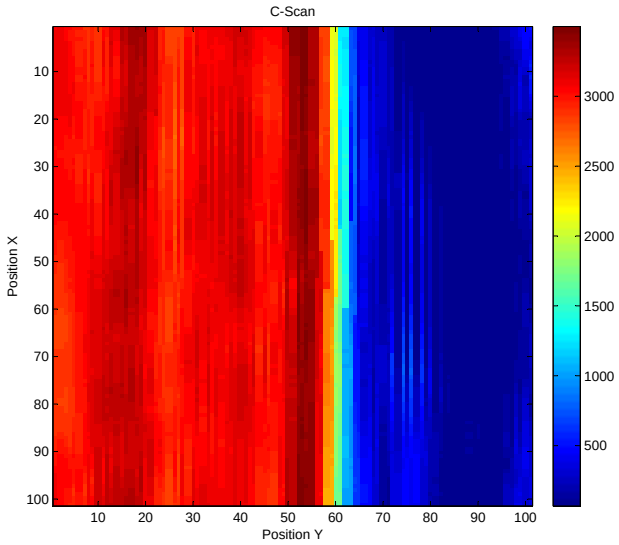

Figure 8: 2D C-scan from the cylindric area of the demonstrator, measured with $110\,\mathrm{kHz}$. On the left Lamb waves could be excited easily, on the right they were damped by elastomer layers on the inner side of the laminate.

effective path velocity of $8\,\mathrm{mm/s}$ was achieved. The C-scan is a winding up from 3D to 2D.

To the right of Position $Y = 60$ an elastomer layer is attached to the inner side of the laminate wall, which damps the Lamb wave almost completely. This happens only if the bonding between laminate and elastomer is closed. Therefore, a method was found for testing the bonding of a layer to the rear side of a CFRP laminate by using Lamb waves.

C. Measurement of a pressure vessel

This is a CFRP-component that was constructed in the frame of the project 'ComBo' (Effiziente Fertigungstechnologie für Composite Boostersegmente). In ComBo lightweight production technologies are studied, which will be necessary for the NGL (Next Generation Launcher), the successor system of the currently used Ariane 5. The task is to reduce mass and production costs of structural components in order to carry a payload to the Earth orbit more efficiently. In practice it is about developing a cost-effective production process for a CFRP-pressure vessel used as a solid fuel booster housing. The vessel which was inspected in this paper was constructed at the Lehrstuhl für Carbon Composites of Technische Universität München after plans of MT-Aerospace Augsburg and handed over to DLR Augsburg for NDI.

Compared to the real size of a pressure vessel, the inspected one is scaled down to one third. It consists of two parts, which together have a length of $3.7\,\mathrm{m}$ and diameters of $1.4\,\mathrm{m}$. Fig. 9 shows the larger part of the pressure vessel ($2.3\,\mathrm{m}$ long) mounted on the TTT. Since the pressure vessel was produced by the same technique like the demonstrator component, it has the same high amount of porosity. The task was a complete inspection of both parts of the vessel, detection of flaws with at least $10\,\mathrm{mm}$ size and visualization in two- and three dimensional C-scans.

However, before doing this, some preliminary test had to be conducted. In contrast to the demonstrator, which has a laminate thickness around $5\,\mathrm{mm}$, the pressure vessel parts have areas with up to $40\,\mathrm{mm}$ laminate thickness (in Fig. 9 at the lower end of the component). Exciting Lamb waves in such laminates was supposed to be challenging and had to be proven first.

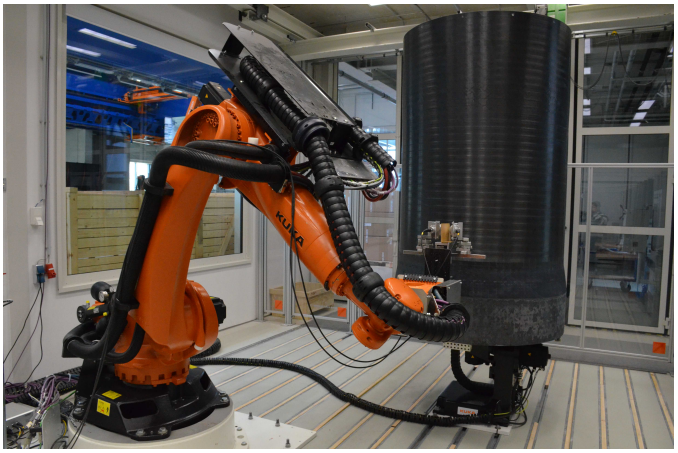

Figure 9: Robot cell at DLR Augsburg with KUKA robot. The longer one of the two parts of the pressure vessel is mounted on the TTT.

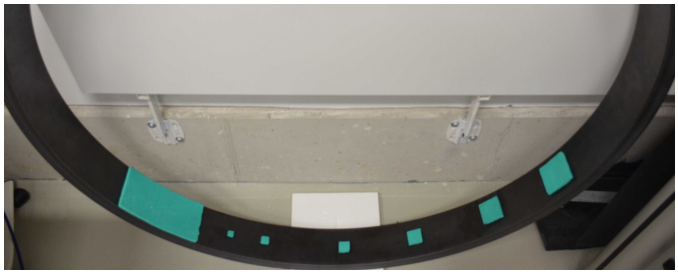

Figure 10: Elastomer layers glued on the inner side oft the test ring for proving the excitation of Lamb waves in a $40\,\mathrm{mm}$ thick laminate.

Although a signal propagating through the laminate was received, it was not clear whether it was a Lamb wave. It could also be a Rayleigh wave, which causes oscillation in the plate only to a certain depth but not throughout the whole thickness. This would be undesirable, since the laminate could not be inspected completely. To get a test component, a ring of $12\,\mathrm{cm}$ height, which was dispensable anyway, was cut from the $40\,\mathrm{mm}$ thick area. As shown in Fig. 10, layers of the same elastomer, which have been used inside the demonstrator (and the vessel) were glued on the inner side of the laminate. In case a Lamb wave could be excited, a damping of the signal was expected as experienced before on the demonstrator. The sizes (in mm) of the elastomer layers are listed in Fig. 11b. In thin laminates this test can be accomplished just by pressing the thumb on the rear side of the laminate.

Fig. 11a displays the resultant C-scan in 3D using $64\,\mathrm{kHz}$ transducers. Fig. 11b shows a two dimensional cutout of the 3D representation. The positions and sizes of the elastomer layers are drawn true to scale in green colour. The layers become visible beginning with a size of $20 \times 20\,\mathrm{mm}$. However, for unknown reasons they cause an amplification of the signal here (red colour corresponds to high amplitude). Nonetheless, the excitation of Lamb waves using $64\,\mathrm{kHz}$ transducers was proven, while this was not possible with 110 and $200\,\mathrm{kHz}$ transducers.

After this test, the measurements on the vessel could be carried out. Because of the size of the vessel it was necessary to increase path velocity and pulse repetition frequency. This could not be achieved in stop & go mode but only through on-the-fly triggering. Therefore, the KUKA technology package 'Fast Send Driver' (FSD) was installed on the robot control unit. The FSD is yet only a prototype, which allows for path-equidistant triggering with rates as high as $1000\,\mathrm{Hz}$. This means triggering along any path, no matter how complicated it is, with very high path velocity, e.g. $2\,\mathrm{m/s}$ with $2\,\mathrm{mm}$ step size. The FSD also performs on-line merging of the ultrasonic data coming from the ACU-testing device with the corresponding position data from the robot/TTT, respectively. This technology is brand new and applied only by very few users worldwide.

In our measurements maximal pulse repetition frequencies

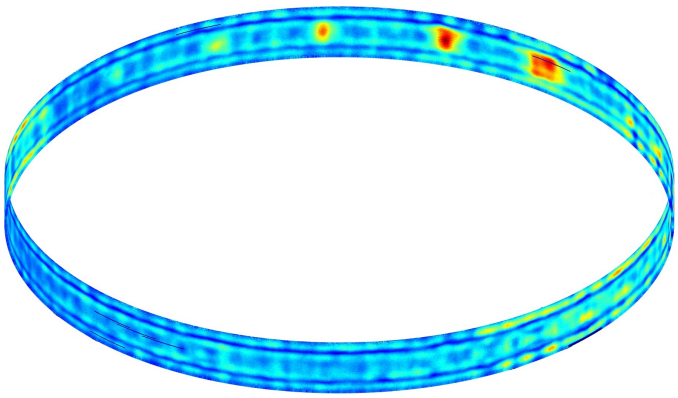

(a) 3D representation

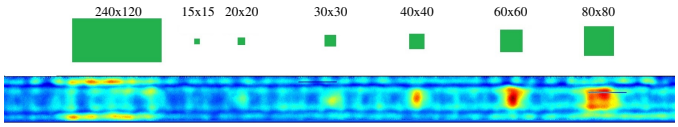

(b) 2D representation

Figure 11: Measurement on the ring with 64 kHz. (a) 3D representation (b) 2D representation. The elastomer layers (sizes in mm) cause an unexpected amplification of the signal, which nonetheless proves the excitation of Lamb waves.

of 115 Hz were triggered. Again using a $2 \times 2\,\mathrm{mm}$ grid yielded a path velocity of $230\,\mathrm{mm/s}$, which is already a decent increase as compared to preceding measurements, although the TTT was rotated only at 50 % speed. The ACU-testing device's maximum pulse repetition frequency is 250 Hz and higher rates are not reasonable since the ultrasonic signal needs a certain time to propagate from the transmitter to the receiver.

Due to the length of the scanning program for such a large component it was created by offline programming (OLP). This was done using DELMIA and FASTSURF. As shown in Fig. 12, the scanning program is simulated in a CAD-like environment containing the CAD of the component or, as it was done in the present case, with a model of the vessel obtained from topographical survey. After simulation the program is transferred to the robot control unit. Principally, the program for the vessel is similar to the one used for the demonstrator except that full rotations are performed now.

After automated measurement of the vessel a huge amount of C-scans had to be evaluated. It is obvious that the evaluation process should be automated as well, because manual evaluation of C-scans is time consuming. This is especially true for such an inhomogeneous material as presented here, where structural indications are more likely to occur. For instance, in some areas of the vessel (not shown in this paper), ending tapes caused structural indications, which should not be confused with flaws.

For obvious reasons only cutouts of the complete C-scans can be shown here. One example with a clear flaw indication is presented in Fig. 13. It visualizes a 100 cm wide and 75 cm high cutout from the cylindric area of the component displayed in Fig. 9 and demonstrates the evaluation process by post processing.

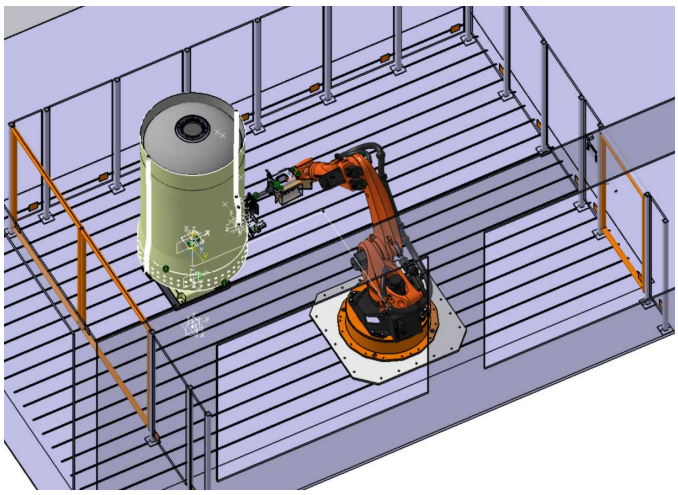

Figure 12: Offline programming of the scanning program for the vessel in DELMIA. The Robot cell and vessel part are displayed in their correct dimensions.

Fig. 13a shows the raw ultrasonic data measured with 64 kHz. This cutout consists of two measurements merged horizontally. In the upper two third the alignment of the tapes along an angle of $\pm 17\,^\circ$ with respect to the horizontal can be identified. Multiple indications appear in the lower right corner. Since they stand out clearly from their surrounding area they can not be ascribed to structural features. Structural features should be more continuous. Probably some kind of cavities have developed by incomplete consolidation during the winding process.

For the evaluation of the raw data, two filters were programmed. The first one calculates the local standard deviation (1σ) of the ultrasonic amplitude. This accommodates both possibilities of amplitude deviation caused by flaws in reflection mode, namely decrease *and* increase. As reference the local mean amplitude is calculated within a square of certain size around the pixel to be evaluated. The mean amplitude determination is moving with its respective pixel. As visible in Fig. 13b, the indication in the lower right corner is accentuated by this operation and its structure and orientation are worked out. The horizonal line accounts for the merging of two measurements and therefore is not a material feature.

Another filter was programmed for applying an amplitude criterium. All local standard deviations exceeding a certain threshold are indicated in a two-colour chart, depicted in Fig. 13c. The multiple indication is now definitely marked as a flaw.

Finally, sizes, coordinates or densities of indications were determined manually. Another filter for this work is not available yet. Basically, it is about the application of a size criterium. Any indication in the two-colour chart exceeding a certain size threshold will ultimately be tagged as a flaw. Its properties should then automatically be exported into a flaw list file, saved on a data base, and be available for process optimization.

Furthermore, work has to be done on developing amplitude- and size criteria, which are less arbitrary like the known

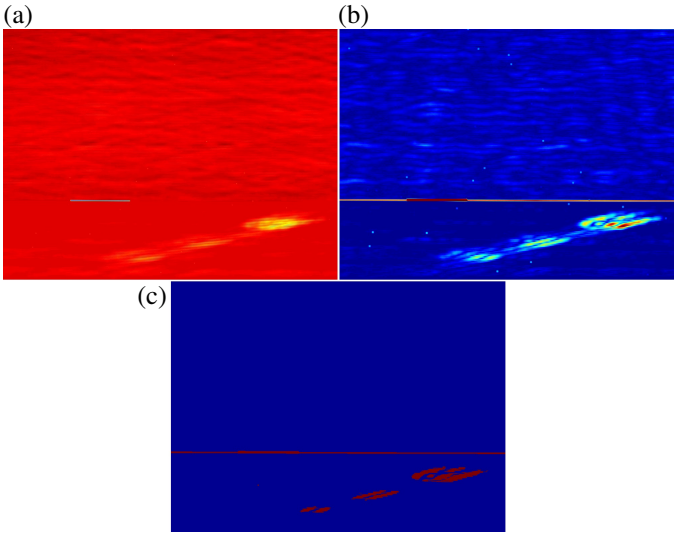

Figure 13: Evaluation of a C-scan cutout of the vessel obtained with 64 kHz transducers. (a) Raw ultrasonic data with multiple indications in the lower right corner. (b) The local standard deviation accentuates the indication. (c) The indication's local standard deviation exceeds the threshold and is hence defined as a flaw.

-6 dB-criterium or the threshold values used in the present work. Threshold values corresponding to a critical stiffness loss must be attained empirically, or better, by finite element method.

IV. Conclusions

Integration of the ACU-testing device into the robot cell and NDI in reflection mode using Lamb waves was successful. Artificial flaws in a flat plate and structure as well as flaws in a pressure vessel could be resolved. Excitation of Lamb waves in a 40 mm thick thermoplastics was proven using 64 kHz transducers. This material contains a high amount of $2-4\,\%$ porosity and therefore could not be inspected with water-coupled ultrasound. Using air-coupled ultrasound instead enabled complete inspection of the component and detection of flaws. A new method for testing the bonding of an elastomer layer to the rear side of a CFRP laminate by using Lamb waves was found.

The scanning of large and curved components was made possible through using a KUKA robot with six axes cooperating with a tilt-turn table with two additional axes. A new endeffector allows for reproducible adjustment of the transducers along four degrees of freedom. Programming of the robot was realized by offline programming. A high pulse repetition frequency of 115 Hz and a path velocity of 230 mm/s were attained by path-equidistant triggering of the air-coupled ultrasonic testing device. Doubling of these values is possible.

The ultrasonic data could be visualized in two- and three dimensional C-scans, resembling the geometry of the inspected components. This was made possible by the swift online-combination of the ultrasonic data with its respective position data. For the evaluation of the data a supportive post processing procedure has been developed, which will be upgraded in the future.

In summary it was shown that NDI using air-coupled ultrasound can play an equivalent and complementary role next to water-coupled ultrasonic testing. The technical progress that was achieved, especially the advances on the automation of this method let its introduction into industrial quality assurance processes appear as possible an desirable.

Acknowledgement

The author is grateful to the colleagues from DLR Augsburg Thomas Schmidt, Dr. Stefan Nuschele, Manfred Schönheits and Somen Dutta as well as to the collaborator from IKT Stuttgart Peter Fey, to Kevin Zang from Inoson GmbH for providing support regarding the ACU-testing device and to Uwe Düfert from MT-Aerospace for his support on the development of the evaluation procedure.

References

[1] J. Schuller, R. Oster, W. Hillger, and J. Bosse, "Luftultraschallprüfung in der Luftfahrt," in *DACH-Jahrestagung 2012 in Graz - Di.3.A.2*, Sep 2012.

[2] M. Rheinfurth, F. Schmidt, D. Döring, I. Solodov, G. Busse, and P. Horst, "Air-coupled guided waves combined with thermography for monitoring fatigue in biaxially loaded composite tubes," *Composites Science and Technology*, vol. 71, no. 5, pp. 600–608, Mar 2011.

[3] M. Luukkala and P. Merilinen, "Metal plate testing using airborne ultrasound," *Ultrasonics*, vol. 11, no. 5, pp. 218–221, Sep 1973.

[4] D. Döring, "Luftgekoppelter Ultraschall und geführte Wellen für die Anwendung in der Zerstörungsfreien Werkstoffprüfung," Ph.D. dissertation, Fakultät Luft- und Raumfahrttechnik und Geodäsie der Universität Stuttgart, 2011.

[5] W. A. Smith and B. A. Auld, "Modeling 1-3 composite piezoelectrics: thickness-mode oscillations," *IEEE Trans Ultrason Ferroelectr Freq Control.*, vol. 38, no. 1, pp. 40–47, Jan 1991.

[6] W. Gebhardt, W. Hillger, and P. Kreier, "Airborne Ultrasonic Probes: Design, Fabrication, Application," in *7th European Conference on Nondestructive Testing*, May 1998, pp. 3098–3105.

[7] I. Viktorov, *Rayleigh and Lamb Waves: Physical Theory and Applications*. Plenum Press, New York, 1967.

[8] M. Luukkala, P. Merilinen, and J. Surakka, "Plate wave resonance - a contactless test method," *Ultrasonics*, vol. 9, no. 4, pp. 201–208, Oct 1971.

[9] I. Solodov, D. Döring, and G. Busse, "Air-coupled Lamb- and Rayleigh waves for remote NDE of defects and material elastic properties," in *10th International Conference of the Slovenian Society for Non-Destructive Testing*, Sep 2009, pp. 37–45.

[10] M. Castaings, P. Cawley, R. Farlow, and G. Hayward, "Single Sided Inspection of Composite Materials Using Air Coupled Ultrasound," *Journal of Nondestructive Evaluation*, vol. 17, no. 1, pp. 37–45, Mar 1998.

[11] M. Castaings and P. Cawley, "The generation, propagation, and detection of Lamb waves in plates using air-coupled ultrasonic transducers," *Journal of the Acoustical Society of America*, vol. 100, no. 5, pp. 3070–3077, Nov 1996.